α-casein micelles-membranes interaction: flower-like lipid protein coaggregates formation

Authors

Sara Anselmo[1], Giuseppe Sancataldo[1], Vito Foderà[2] and Valeria Vetri[1]*

Affiliations

[1]Dipartimento di Fisica e Chimica – Emilio Segré, Università degli Studi di Palermo, Viale delle Scienze ed. 18, 90128 Palermo, Italy

[2]Department of Pharmacy, University of Copenhagen, Universitetsparken 2, 2100 Copenhagen; Denmark

*Corresponding author: valeria.vetri@unipa.it

Keywords: casein, micelles, protein-membrane interactions, fluorescence, RICS.

Abstract

Environmental conditions regulate the association/aggregation states of protein molecules and their action in cellular compartments. Analysing protein behaviour in presence of lipid membranes is fundamental for the comprehension of many functional and dysfunctional processes. Here, we present an experimental study on the interaction between model membranes and α-casein.

α-casein is the major component of milk proteins and it is recognised to play a key role in performing biological functions. The conformational properties of this protein as well as its capability to form supramolecular structures, like micelles or irreversible aggregates, are key effectors in both functional and pathological effects.

By means of quantitative fluorescence imaging and complementary spectroscopic methods, we were able to characterise α-casein association state and the course of events induced by pH changes, which regulate the interaction of this molecule with membranes. The study of these complex dynamic events revealed that the initial conformation of the protein critically regulates the fate of α-casein, the size and structure of the newly formed aggregates and their effect on membrane structures. Only protein molecules organized in micellar structures are found to severely modify membrane morphology and fluidity. The membrane structure rigidity is found to increase, and protein lipid flower-like co-aggregates are formed with protein molecules localised in the external part.

1. Introduction

Folding, aggregation and interaction of proteins with membranes are at the basis of their functional and dysfunctional activity[1–3]. These phenomena occurrence and evolution are regulated by the balance between general dominant forces as electrostatic, hydrophobic, hydrogen bonding and Van der Waals'. These interactions are dynamically involved in protein's fate and are regulated by micro-environmental properties[4–6]. Cell functions, which most often are carried out within membrane compartments or in their close proximity, often require protein structural reorganization and may occur in close interaction with the lipid bilayer[3,7].

Caseins are relatively small milk proteins (molecular mass in the range of 25 kDa) which belong to the family of intrinsically disordered proteins (IDPs)[8]. They consist of different components namely α_{s1}-, α_{s2}-, β-, and κ-caseins, the main one being α_s (which includes α_{s1} and α_{s2} caseins)[9,10]. These components differ in their amino acid, phosphorus and carbohydrate content, but all of them present an amphiphilic structure[11]. Due to the amphiphilic property, caseins exhibit a strong tendency to self-aggregate into supramolecular structures, and, specifically, into the form of micellar structures which in aqueous solution are held together by the balance of hydrophobic, hydrogen and electrostatic interactions[9,12]. The interaction of casein supramolecular structures with biological membranes is involved in their trafficking within the cells[13].

Among caseins' family, α-casein is one of the most studied and it is thought to have a central role in micelles formation and in the transport process within the secretory pathway of mammary epithelial cells[13,14]. It is a 23.5 kDa protein and its isoelectric point is in the range of 4.4-5.3[15]. At alkaline pHs, between pH 7.4 and pH 10, this protein is characterized by an overall low hydrophobicity, and by a net negative charge[16] that induces the protein to unfold into an open structure characterized by a random coil conformation[17]. In these conditions, α-casein possesses a peculiar aggregative behaviour and it is prone to interact with ligands and lipid interfaces in vivo, including biological membranes[14]. By lowering the solution pH to values below the pI, the net positive charge of casein molecules together with hydrogen bonds and hydrophobic interactions allows casein chains' folding into more structured conformations like α-helixes and β-sheets[17]. Importantly, α-casein molecules were found to associate in micellar structures whose compactness, hydrophobicity, and diameter depend on environmental conditions: i.e alteration of the pH may lead to a change in micelle size and a decreased stability[16,18].

The interest in casein micelles is multifold, ranging from basic to applied sciences. The main physiological functions of micelles are related to the supply of ions such as calcium and phosphate[14] to neonates and to the prevention of calcification of the mammary gland[9]. Notwithstanding the large number of studies, the structure and the stability of casein micelles in different environment is still highly debated[19,20]. For example, there are controversial opinions on the stability of micelles in alkaline solutions. Indeed, for several decades, it has been widely accepted that alkaline pH disrupts casein micelles but recent results have demonstrated their resistance to these pH values[21–23]. Furthermore, the assembly of casein micelles and their binding to the membranes has been related to functional transport phenomena from endoplasmic reticulum to Golgi apparatus making the analysis of the interaction of casein structures with biological membranes of an undoubted relevance in understanding functional casein trafficking in cells[14,24]. Interestingly, due to their ability to self-assembly and disassembly by changing the pH, they were proposed as emerging biomaterials for drug delivery[25–27]. Specifically, micelle structures have been used for controlled release of hydrophobic bioactive components (such as vitamins) and/or hydrophilic molecules that can be embedded in these nano-supramolecular structures[28]. Caseins distinctive structural properties of IDPs and the capability to form amyloid fibrils makes also them an interesting model system in relation to the analysis of potentially pathological protein-membrane interactions[29–31]. The ability of α-casein in binding membranes seems to be related to the antibacterial activity of short peptides isolated within the sequence of this protein[32,33].

In the present study, we highlight key events and species occurring upon interaction of α-casein with negatively charged model membranes thanks to spatially resolved analysis, provided by advanced microscopy that overcomes the limitations of bulk experiments where key events and protein intermediate states, occurring upon interaction with membranes, are often masked due to the large heterogeneity of the sample in terms of number of species involved (e.g., different aggregation states, protein-lipid co-aggregates etc.) and of their spatial distribution[34]. By means of spectroscopic methods, fluorescence imaging and Raster Image Correlation Spectroscopy (RICS), we analysed this highly complex and spatially heterogeneous phenomenon, which involves i) the protein' structural changes and modification in the association states ii) membranes morphology changes and iii) solvent effects.

Specifically, in this study the interaction between POPC:POPG giant vesicles (GVs) and α-casein has been analysed using as starting points two casein molecular states:

micelles stabilised at pH 2 and casein in its native conformational state at pH 7. Our results reveal that the initial state of the protein establishes the course of events that occur upon changes of pH and involve both the aggregation processes of casein molecules and their interaction with membranes. The two samples' states induce, at the same final conditions, a distinctly different effect on the morphology and stiffness of the membranes. These observations may be essential to understand the possible functional, pathological or therapeutical properties associated to α-casein proteins.

2. Materials and Methods

2.1 Materials

α-casein (≥ 70 %, C6780), 2-Oleoyl-1-palmitoyl-sn-glycero-3-phosphocholine (≥ 99 %, POPC-42773), 2-Oleoyl-1-palmitoyl-sn-glycero-3-phospho-rac-(1-glycerol) sodium salt (≥ 98 %, POPG-63371), 6-dodecanoyl-2-dimethylaminonaphthalene (≥ 97 %, Laurdan-40227) and dimethyl sulfoxide (DMSO-1029521000) were purchased from Sigma Aldrich. Alexa Fluor 488 NHS ester (A20000) was purchased from Thermo Fisher Scientific.

2.2 α-casein samples preparation

The aggregation states of bovine α-casein, including α_{s1} and α_{s2} casein, at pH 2, was studied and compared to the one at pH 7. Protein was dissolved to a final concentration of 4 mg/ml in 25 mM HCl with 100 mM NaCl 0.1 M (pH 2), or in 20 mM potassium phosphate buffer (pH 7) and filtered through 0.2 μm cellulose acetate membrane filters (VWR International, 514-0060). Protein concentration was determined by absorption, by means of a UV–Vis spectrophotometer (Jasco V-760), using an extinction coefficient ε_{280nm} = 0.8 ($ml \cdot mg^{-1} \cdot cm^{-1}$)[35].

2.3 Giant Vesicles preparation

Phospholipid Giant Vesicles (GVs) were prepared mixing POPC and POPG in a 2:1 molar ratio in 3:2 chloroform:methanol solution. Using a rotary evaporator, 500 μL of lipids solution was dried to form a thin lipid film. After overnight drying, lipids were hydrated with buffer phosphate 20 mM, pH 7. Resulting sample shows a

heterogeneous distribution of multilamellar giant vesicles with diameter of several micrometers. After liposomes formation, sample was diluted 1:10. A stock solution of Laurdan (100 μM) was prepared in DMSO and stored protected from light exposure. Laurdan solution was added to dilute GVs in a probe-lipid molar ratio of 1:500 and left to equilibrate for 3 hours before measurements.

2.4 Circular dichroism measurements

CD spectra of 36 μM α-casein samples in pH 2, pH 7 and pH 5.3 solutions were recorded on a Jasco J-715 spectropolarimeter in the far-UV region (194–260 nm), using quartz cuvettes with a path length of 0.5 mm. For each spectrum, three accumulations have been acquired, with data interval 0.2 nm, bandwidth 1 nm, scan speed 50 nm/min. All spectra have been acquired at room temperature.

2.5 Steady state fluorescence emission spectra

Fluorescence measurements were acquired at room temperature using a Jasco-FP-8500 spectrofluorometer equipped with a Jasco ETC-815 Peltier as temperature controller in 1 cm path length quartz cuvettes.

2.5.1 Pyrene measurements

Pyrene is a neutral hydrophobic fluorescent probe characterized by a very low solubility in water (0.7 μM) and, as a result, it is selectively solubilized in the hydrophobic region of coexisting micro-phases in aqueous medium. The analysis of its vibronic fluorescence spectrum, in particular, the ratio of the first peak at 373 nm to the third peak at 393 nm (I_1/I_3), has been widely used to monitor the polarity of the hosting microenvironments[18].
The emission spectra were measured in the range 350–550 nm with the excitation wavelength being 330 nm. The Pyrene concentration was 1.0 μM.

2.5.2 1-anilino naphthalene-8-sulfonate (ANS) fluorescence

1-anilino naphthalene-8-sulfonate (ANS) is an anionic probe that has been selected to study the surface hydrophobicity of the samples. ANS fluorescence is strongly dependent on the polarity of the environment[18]. ANS emission spectra were acquired in the range 400-650 nm using λ_{exc}= 350 nm with an excitation bandwidth of 5 nm, an emission bandwidth of 5 nm, a response time of 1 s, data interval of 0.5 nm, and a scan speed of 100 nm/min. The ANS concentration was 9.0 μM.

2.5.3 Laurdan fluorescence emission

Laurdan fluorescence emission and, in particular, its generalized polarization (GP) were used to investigate the effect of casein at pH 2 on POPC:POPG vesicles. Fluorescence emission spectra were acquired in the range 370–650 nm as a function of time every 5 minutes after casein addition to a final concentration of 36 μM. Excitation wavelength was λ_{exc} = 380 nm and emission bandwidth was 5 nm, response time 1 s, data interval of 0.5 nm and scan speed of 100 nm/min. According to Parasassi et al.[36], the Generalized Polarization (GP) is defined as:

$$\mathrm{GP} = \frac{(\mathbf{I_{440}} - \mathbf{I_{490}})}{(\mathbf{I_{440}} + \mathbf{I_{490}})} \qquad \mathbf{1}$$

where I_{440} and I_{490} are the emission intensities at 440 and 490 nm respectively. Laurdan emission spectrum is centred at about 440 nm in the membrane gel phase and at about 490 nm in the membrane liquid crystalline phase[37,38]. Due to Laurdan properties, GP value analysis allows determining the phospholipid phase state as well as the variations in membrane fluidity due to changes in membrane water content. Control measurements were performed adding the same quantity of buffer solution to vesicles samples (see supplementary Fig.S1).

2.6 Raster Imaging Correlation Spectroscopy (RICS)

α-casein was labelled according to a standard procedure[39] and separated in a Sephadex G-50 column equilibrated with phosphate buffer 20 mM at pH 7. To further eliminate free dye, the labelled protein was centrifuged three times (13000 rpm, 10 min) with Milli-Q water to wash it using 10 kD centrifugation filters. The concentration of the dye was determined by absorbance at 503 nm using an extinction coefficient of 73000 cm^{-1} M^{-1}. For RICS experiments, freshly prepared casein (4 mg/mL, pH 2) was

mixed with casein-Alexa$_{488}$ (final concentration 52 nM). Aliquots of samples at pH 2 and 7 containing Alexa$_{488}$-labelled protein were added to chambered cover glasses (Lab-Tek II Nunc) (final concentration of Alexa$_{488}$-labelled protein 13 nM). Images were acquired in single channel with an Olympus FluoView1200 confocal laser scanning microscope (Olympus, Tokyo, Japan) using an UPLSAPO 60 × 1.2 NA objective using chambered cover gasses (Lab-Teck II Nunc).

Alexa$_{488}$ fluorescence was excited using the 488 laser line and acquired in photon counting mode using a 520 nm−620 nm emission filter. For RICS analysis, 70 frame image stacks were acquired (256 × 256 pixels) at different dwell time of 8, 10, 12.5, 20 μs/pixel. The electronic zoom was set at ×16.3 (pixel size of 0.05 μm). Analysis was performed using the RICS algorithm of SimFCS program. RICS autocorrelation function has been fitted using the diffusion model to calculate the characteristic parameters of the process: the amplitude of the correlation function G_0 and the diffusion coefficient D. The excitation volume was calibrated by using a solution of Alexa$_{488}$ in water containing and setting the diffusion coefficient to 350 $\mu m^2/s$[40]. For this measurement, the dwell time was reduced to 4 μs/pixel. Radius calculations were performed with Stokes−Einstein equation:

$$D = \frac{\mathrm{kT}}{6\pi\eta\mathrm{R}} \qquad \mathbf{2}$$

where *k* is the Boltzmann constant, T is the temperature (298 K), D is the calculated diffusion coefficient, η is the viscosity of the media (1.16 cP), and R is the radius.

2.7 Protein-membrane colocalization experiments

GVs labelled with Laurdan were imaged before and after addition of α-casein (36 μM) stained with Alexa$_{488}$. 500 μL aliquots were deposited in Chambered Coverglass (Nunc Lab-Tek II) and imaged using a Leica TSC SP5 confocal laser scanning microscope, with a 63× objective, NA = 1.4. Scanning frequency was 400 Hz. 1024 × 1024 pixel images were acquired in a sequential mode of three channels: Alexa$_{488}$ emission was acquired in the range 510-600 nm, using λ_{exc} = 488 nm; Laurdan emission was acquired in the range 430-450 nm (blue channel) and in the range 475-495 nm (green channel) using 2-photon excitation (Spectra-Physics Mai-Tai Ti:Sa ultra-fast laser), at 780 nm.

3. Results

3.1 Characterization of α-casein samples at acidic and neutral pH

In Fig.1.a) and 1.b) results of RICS analysis on 36 μM α-casein samples (containing $Alexa_{488}$ labelled protein at 13 nM) in HCl-NaCl solution at pH 2 and in phosphate buffer at pH 7 are shown. These measurements are aimed at characterising the aggregation state of the two samples and to assess the potential presence of supramolecular assemblies. In panel 1.a) 256×256 pixel size representative images are reported together with the spatial autocorrelation functions and the fitting, obtained from the analysis of the two samples. Fluorescence images do not reveal the presence of structures with characteristic size above diffraction limited resolution of the microscope (~200 nm) so that uniform fluorescence is measured. In line with this observation, the shape of the autocorrelation functions is characteristic of free diffusion. Several measurements were performed on multiple areas of the samples and diffusion coefficients obtained from RICS analysis are reported in panel 1.b). A critical difference is found between the two samples, being the diffusion coefficients in the sample at pH 7 significantly larger than the one in sample at pH 2. The measured diffusion coefficient for α-casein pH 7 sample is about 60.0 $\mu m^2/s$ and, in line with literature, stems for the dominant presence of proteins in the monomeric form or self-associated into dimeric or tetrameric structures[41].

In casein samples at pH 2 the measured D is about 31.0 $\mu m^2/s$, indicating the presence of large slow diffusing aggregates. This result is in accordance with data reported in literature showing that α-casein has a great tendency to form micelles (about 10 subunits or more) at this pH and, accordingly, this result indicates the presence of supramolecular micellar structures[18].

In order to verify if the protein exists in different aggregation states (i.e. different diffusion coefficients), we used the moving average (MAV) subtraction tool (supplementary Fig.S2). MAV in RICS analysis is the subtraction of the signal of the immobile/slowly diffusing species that contribute to fluctuations in the same pixel for a time longer than the acquisition time of multiple frames[42,43]. The length of the MAV can be useful to emphasize processes on different timescales, and in particular to select the slow processes affecting RICS autocorrelation function. Our data reveal that the autocorrelation functions, varying the MAV, are not affected in their shape meaning that the sample is characterised by homogeneous size distribution over the observed timescale.

Panel 1.c) shows the far UV CD spectra of α-casein at pH 7 and pH 2. CD signal reflects peptide backbone organization and it is widely used to analyze protein secondary structures[44]. It is known that pH is an important factor determining protein structure and that its alteration disrupts electrostatic interactions between charged residues that form salt bridges in a polypeptide chain, thus altering its native folded structure. In line with data reported in the literature, at pH 7 α-casein presents a CD spectrum characteristic of a high content of α helices and random coil structures. At acidic pH the shift of the first minimum in ellipticity from 200 to 206 nm accompanied by spectral changes is indicative that random coil conformations are replaced by ordered conformations like helices and intermolecular β-sheets. In Fig.1.d) we report the fluorescence emission spectra (λ_{exc} = 330 nm) of Pyrene dye added to the two casein samples; the overlapped spectra of Pyrene in aqueous solution at pH 2 and 7 are also reported for comparison. These measurements are aimed at corroborating the idea that micelles are present in the sample at pH 2 and that only small fraction of casein molecules are organised in micelle structure at neutral pH. It is known that interactions between casein molecules might already take place in the Endoplasmatic Reticulum, characterized by neutral pH, forming submicelles and then proceed to micelles formation in the late secretory pathways where the pH values become more acidic[45,46]. Pyrene has been already used to probe the existence of casein in micellar state and to investigate the influence of pH on micelles properties[18]. Variation in the fluorescence intensity ratio between the peaks centered at 373 nm and 393 nm (I_1/I_3) is considered an indicator of the presence of these structures. In particular, the presence of micelles in solution induces the decrease of the I_1/I_3 ratio. The reported data show that Pyrene in aqueous solution at both pHs is characterized by a peak ratio I_1/I_3= 1.10 $\pm$ 0.01. In the presence of α-casein this value decreases to 1.06 $\pm$ 0.01 at pH 7 and to 1.02 $\pm$ 0.01 at pH 2. This result reveals a more hydrophobic environment in the case of casein at pH 2 and support the hypothesis of a dominant presence of micellar structures at acidic conditions. We report in Fig.1.e) the fluorescence emission spectra (λ_{exc}= 350 nm) of ANS dissolved in the two samples at pH 2 and 7 at the same concentration. As it is well known, ANS fluorescence is strongly dependent on the polarity of the local environment around the chromophore[47]. In water, the emission is relatively weak, with a maximum around 520 nm. Upon binding to hydrophobic patches of proteins, the fluorescence spectrum is blue-shifted with a maximum around 470 nm and the emission intensity is increased[18]. The reported spectra are normalized for their absorbance at 275 nm. They show a high fluorescent

emission with a maximum centered at 470 nm for ANS added to casein sample at pH 2, while a lower fluorescent emission, with a maximum centered at 480 nm, for ANS added to casein sample at pH 7. Also in this case, results are in line with previously reported literature indicating a higher affinity of ANS for casein in acidic conditions suggesting the presence of stable and compact micellar structures[16].

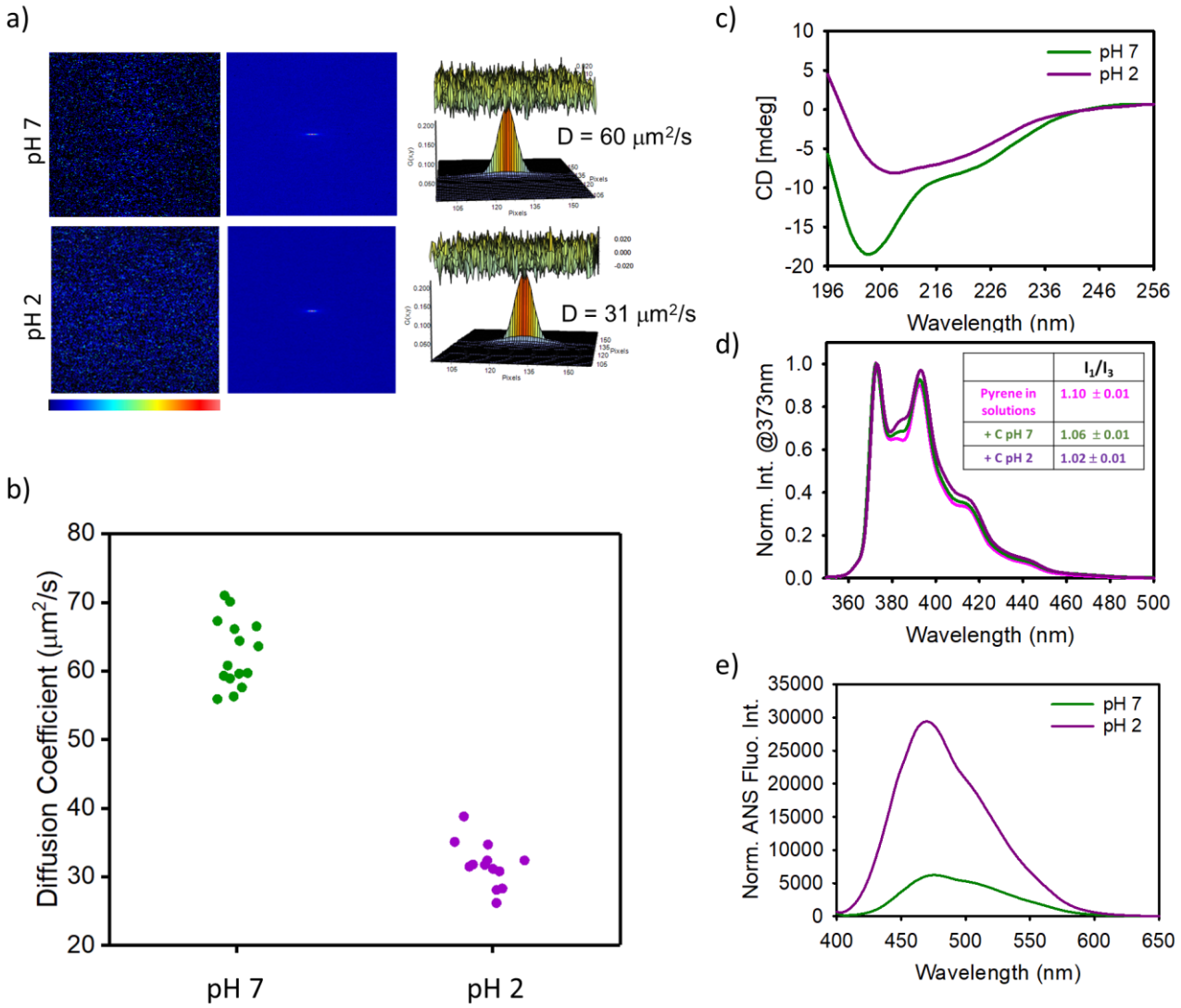

Fig. 1 (a) Representative 256 × 256 confocal images of 36 μM α-casein in pH 7 (20 mM phosphate buffer) and pH 2 (25 mM HCl, 100 mM NaCl) labelled with $Alexa_{488}$ (13 nM). Spatial autocorrelation function of the two samples and their respective fits are also reported. The diffusion coefficients (D) are 60 $\mu m^2/s$ for α-casein pH 7 and 31.8 $\mu m^2/s$ for α-casein pH 2. (b) Diffusion coefficient distribution of the two samples. (c) Far-UV (194-260 nm) CD spectra of 36 μM α-casein pH 7 and α-casein pH 2. (d) Fluorescence emission spectra (λ_{exc} = 330 nm), in the range 350–550 nm and normalized to their value at 373 nm, of Pyrene (1×10^{-6} M) in solution pH 7 and solution pH 2, both in absence (overlapped spectra) and in presence of casein. The results of the ratio between the first and the third peaks are reported in the table in the inset. (e) ANS fluorescence emission spectra (λ_{exc}= 350 nm, range 400-650 nm) in presence of 36 μM casein pH 7 and pH 2. All these experiments were performed in triplicates.

Previous results show that α-casein can form micelles and that the stability of these structures is pH-dependent, being their formation significantly favoured at acid pH. Recent studies have shown that micelles destabilisation is a pH-driven process. Changes in the surface charge and the consequent conformational changes, modulated by electrostatic and hydrophobic interactions, may favour or disfavour the formation and or the compaction of micellar structures[11,16]. In particular, it is possible to infer that at pH 2, i.e. below the isoelectric point, many amino acid residues in casein, such as lysine, arginine and histidine are protonated and since the ability of H^+ to form hydrogen bond is much stronger than that of the neutral H atoms, there exist strong hydrogen bonds between casein molecules. In addition, the cationic side chains of these amino acids could be involved in the so-called cation–π interactions with the aromatic side chains of phenylalanine, tyrosine, or tryptophan residues. All these interactions together with the hydrophobic ones may play a key role in the self-assembly of casein[10]. In line with these considerations, the global observation of data in Fig.1 makes clear the nature of the two samples in the selected experimental conditions, revealing that α-casein monomers, with α-helical and random coil structure, constitute the dominant population in sample at pH 7. At pH 2, compact α-casein micellar structures are mainly present stabilised by intermolecular β-structures whose formation is favoured by acidic pH.

3.2 Casein micelles are not stable structures to pH changes

The conformational flexibility of casein proteins represents a really good chance to study in vitro the molecular events controlled by pH changes. Indeed, pH alterations could force conformational modifications and aggregation/ disaggregation processes whose occurrence may be related to different biological effects. This is common in intracellular environment where pH changes are known to affect many cellular properties as they induce changes in membrane potential, in the diffusion or action of different molecules, in functional interactions, in the state of polymerization of the cytoskeleton etc. To regulate cellular functions, many organelles lysosomes, mitochondria and endosomal vesicles act as functional compartments, which maintain their internal pH different from the cytoplasmic one[46,48].

Within this scenario, as a model we analyze the fate of the two samples characterized at pH 2 and pH 7 when the pH of the solution is brought to the isoelectric point of the

protein at pH 5.3. This is aimed at revealing the role of the electrostatic interactions in protein stability, at highlighting key events and protein states and at focusing on how the "sample's history" affects the protein-protein and protein-environment interactions. In other words, we will verify that environmental changes induced modifications in protein structures and that following intermolecular interactions take memory of the initial environmental conditions and protein aggregation state.

Fig.2.a) shows 256 × 256 pixel representative confocal fluorescence microscopy image of 125 µL of casein at pH 2 (final concentration 36 µM labelled with $Alexa_{488}$ (13 nM)), added to 375 µL pH 7 solution to reach a final pH of 5.3. At this pH, large amorphous aggregates are visible. Near the pI of the protein, the net charge on protein becomes zero and the absence of any net charge on molecules leads to a minimum in the intramolecular charge repulsions. In these conditions, the lack of repulsive interactions allows neighbouring caseins to coalesce and form aggregates that precipitate in micron scale aggregates. Therefore, while at acidic pH the casein molecules are held together preferentially by hydrogen bonds and cation–π interactions, at pH 5.3 the main forces involved are the hydrophobic ones. We report in Fig.2.b) RICS analysis of casein micelles aimed at highlighting what happens to the protein during this pH change. 256 × 256 pixel size representative images of 36 µM micelles containing 13 nM component of protein labelled with $Alexa_{488}$ together with the representative spatial autocorrelation function and the fitting calculated in a 64 x 64 ROIs. As can be seen, an appreciable inhomogeneity in fluorescence signal attributed to labelled proteins is found. This suggests the coexistence of multiple species in solution and the presence of fluorescent protein aggregates. For this reason, to analyse RICS data MAV subtraction was used in order to eliminate the contribution of the immobile molecules and to emphasize processes on different timescales. The MAV=10 used for this analysis, given the experimental conditions (frame time = 1.2 s), corresponds to a residence time of ∼10 s. The diffusion coefficients distributions of these species obtained by RICS analysis in different areas of the sample are reported in Fig.2.c). Data prove that when the sample is brought to pH 5.3 from micellar state, it shows a heterogeneous distribution. In particular, large low diffusing protein aggregates with D = 2 ± 2 $\mu m^2/s$ are formed. In the same sample, other smaller diffusing species are found characterized by diffusion coefficient values ranging from 17 $\mu m^2/s$ to 70 $\mu m^2/s$. The latter is comparable to the diffusion coefficient of casein pH 7 (Fig.1.b)). This means that, as expected, micelles are not stable structures but undergo a partial disassembly and reassembly process when bring to pH 2 to pH 5.3.

Fig.2.d) shows the far-UV CD spectra of α-casein before and 15 minutes after pH change from pH 2 to pH 5.3. These bulk measurements show a significant change in spectral shape due to pH change and a decrease in magnitude when the protein is at pH 5.3. In particular, the first peak at 206 nm decreases in magnitude, becoming almost equal to the second minimum at 222 nm. This suggest that the sample loses its initial structure and undergoing structural changes toward α-helices structures.

ANS spectra reported in Fig.2.e) reveal that a critical reduction in intensity and red shift occur when the sample is titrated at pH 5.3. Specifically, the decrease and the red shift (peaks are now centred at 480 nm) of ANS spectrum in presence of casein at pH 5.3 could be due to a different exposure of the casein hydrophobic patches to the dye and/or the decrease of the electrostatic interactions between the positive charges of casein and ANS negatively charged. Thus, ANS at pH 2 was in close interaction with micellar structures, following the pH changes the affinity or the number of the binding sites for this dye result to decrease.

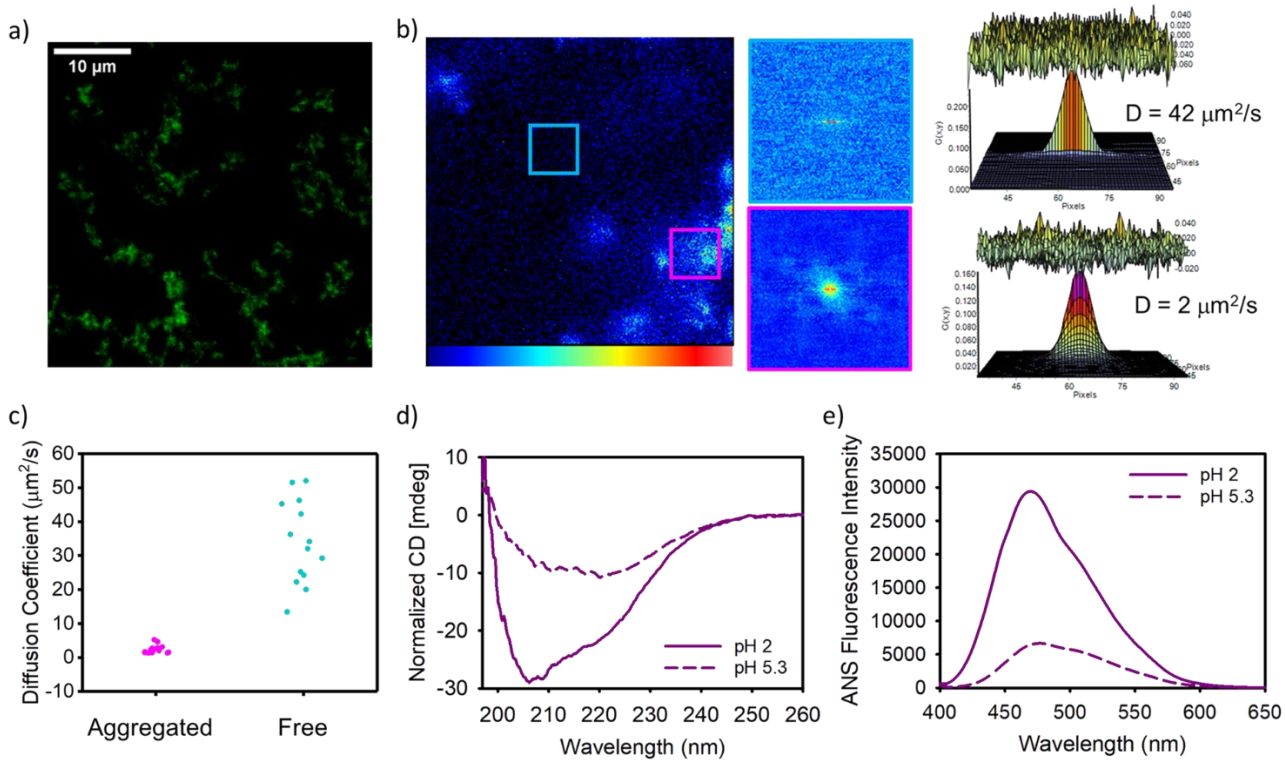

Fig. 2 (a) 256 × 256 representative confocal fluorescence microscopy image of 36 μM casein in pH 2 added to pH 7 solution reaching a final pH of 5.3. Casein molecules at pH 5.3 assemble together in amorphous larger aggregates. (b) Representative 256 × 256 confocal images, the corresponding spatial autocorrelation functions of areas marked (64 × 64) and the respective fits of 36 μM casein in pH 2 added to pH 7. Spatial autocorrelation function calculated subtracting the immobile fraction with MAV =10. Large amorphous aggregates characterized (D = 2 ± 2 $\mu m^2/s$) coexist with smaller species (D = 42 ± 10 $\mu m^2/s$). (c) Diffusion

coefficient distribution of the aggregated part and free one in solution. (d) Far-UV (194-260 nm) CD spectra and (e) ANS fluorescence emission spectra (λ_{exc}= 380 nm, range 400-650 nm), normalized by absorbance, of 36 μM casein brought at pH 5.3 (dotted lines) in comparison with casein in pH 2. All these experiments were performed in triplicates.

Summing up, by changing solution conditions, electrostatic interactions between protein molecules are critically modified. The observation that micelles quickly disassemble confirms the idea that electrostatic controls the stability of micellar structures. At pH 2, many amino acid residues are protonated so that intermolecular H-bonding capability is increased favouring micellar structures formation. Increasing the pH, the ionization of acidic side groups of aminoacids like aspartic acid (Asp) and glutamic acid (Glu) of the proteins increases, whereas that of the basic side groups decreases; as a result, the net-negative charge and hence intermolecular repulsion increases, which may lead to the loose structure of the casein micelles. At pH 5.3, value near the isoelectric point, the lack of net charge on protein molecules induces an extinction of the repulsive interactions between neighbouring caseins that then coalesce to form aggregates. Interestingly, by repeating the same experiments series using the sample at pH 7 corrected towards pH 5.3, small CD spectral changes are in line with the one observed in the literature for sample at similar pH values[17] (data not shown) and macroscopic aggregation is not observed (data not shown but confirmed in the follow by results illulated in Fig.5.a)).

3.3 α-casein-membrane interactions depends on the initial aggregation state

The study of disassembly and reassembly phenomena aims to highlight the events underling both physiological and pathogenic processes. Depending on environmental conditions (i.e. pH, temperature), proteins can go towards aggregation processes, which may be followed by abnormal interactions with the environment. It is known that α-casein reacts very rapidly to environmental changes and it is able to interact with multiple target molecules and in particular with lipid membranes[13,14,45,49]. In addition to the interest regarding the general nature of the interactions involved in these phenomena, it should be mentioned that the functional casein transport efficiency from the ER to the Golgi apparatus is strongly affected by the protein aggregation state and by its interactions with membranes[14,49].

Data reported in the following highlight the events occurring when α-casein micelles are brought at the protein isoelectric pH in a sample containing model membranes. In Fig.3.a) is reported a schematic representation showing fluorescent casein micelles, prepared at pH 2, added to a solution containing POPC:POPG GVs labelled with Laurdan to a final pH of 5.3. In Fig.3.b) bulk Laurdan fluorescence analysis of the sample is reported. Laurdan is a fluorescent dye widely used to monitor membrane organisation changes in term of hydration and fluidity of phospholipid bilayers[50–52]. The fluorescence signal of this molecule depends on the membrane phase (e.g., local and translational mobility) so that changes from liquid-ordered phase to liquid-disordered phase induce a shift of the Laurdan spectrum from 440 nm to 490 nm. The quantification of these spectral changes is usually addressed by the generalized polarization GP, which allows to distinguish between liquid ($-0.3 < GP < 0.3$) and gel phase ($GP > 0.4$) of the membranes[37]. The time evolution of Laurdan GP is reported in Fig. 3.b). In line with literature, membrane is initially found in the liquid phase (GP ~ -0.04), a more accessible state to the solvent. After casein addition, GP increases indicating a progressive change in membrane fluidity towards a more ordered phase. In particular we assist to an abrupt increase of the GP value from -0.04 to 0 in the first 5 minutes and a slow and more or less linear growth of the GP value to 0.02 in the following 25 minutes. After 30 minutes from the addition of α-casein the GP value seems to have reached the stability.

A previous study, aimed at evaluating the role of phase and charge of the phospholipid membrane caused by its interaction with caseins, revealed that casein particles interacted with bilayers in their liquid state and not with solid phase bilayers[13]. In the last case, compact lateral organization of the phospholipids probably prevents penetration of the protein. The presented results show that the membrane stiffening is mild but significant and that protein interaction induces dehydration of lipid bilayers resulting in more rigid membranes. In order to verify the single effect of pH on membranes stiffening, a control measurement adding the same quantity of solution at pH 2 (without α-casein) to liposomes was carried out (see supplementary Fig.S1), showing that it does not significantly affect membrane rigidity.

Fig. 3.c) shows representative fluorescence microscopy measurements on POPC:POPG giant vesicles stained with Laurdan (magenta channel) before and after the addition of 36 μM α-casein labelled with $Alexa_{488}$ (13 nM) (green channel), initially in the micellar state at pH 2 towards a final pH of 5.3. $Alexa_{488}$ fluorescence is used to follow the fate of protein, which is found to interact with GV's structures. In the absence of protein, liposomes present a regular shape, with almost spherical

morphology; the sample shows a detectable heterogeneity in terms of size (ranging from 2 to 10 μm) and in bilayer organisation. After the addition of labelled protein, the spatial overlap between the fluorescence signals acquired in the two channels is clearly evident thus indicating that the protein interacts with GVs. Images also reveal that casein interacts only with the outer part of the membranes; the green signal is revealed only at the edges of GVs, while no protein is localised in the core. It is clearly evident that co-localisation occurs (white areas) between lipid layer and proteins, suggesting that casein molecules are not only adsorbed on membranes but they insert in the membrane. This induces a dramatic membranes remodelling, leading to flower-like structures. The changes in membrane rigidity found by bulk measures (Fig.3.b)) are likely to be localised on interactions sites where protein is localised in the external part of the vesicles: after casein addition, liposomes seem to semi-crystallize into co-aggregates with spherical symmetry constituted by a central lipid core and an external shell with hybrid lipid- casein composition. Other structures are also present in the sample that appear only made of protein molecules (green micron scale structures, highlighted by dashed box).

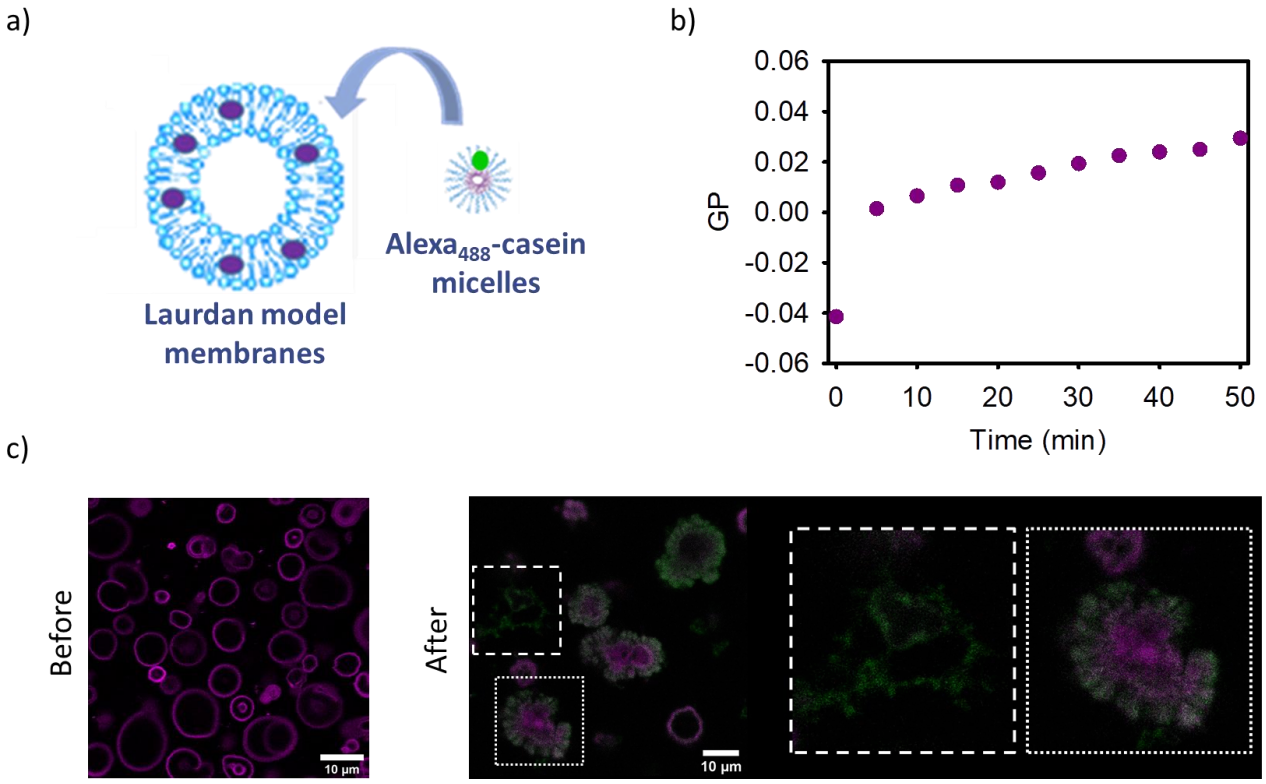

Fig. 3 (a) Schematic representation of $Alexa_{488}$-micelle aggregates and POPC:POPG model membrane labelled with Laurdan. (b) Time evolution of GP ratios obtained from the analysis of Laurdan fluorescence spectrum variations, measured in bulk, after the addition of casein micelles. (c) 1024 X 1024 pixels representative

fluorescence image shows POPC:POPG vesicles, stained with Laurdan (magenta), before and after the addition of 36 μM $Alexa_{488}$-micelles. In presence of 36 μM $Alexa_{488}$-micelles, the overlap of two colors indicates protein-vesicles co-localization that induces a clearly membrane morphology modification. The magnifications show casein aggregates formed at pH 5.3 and the liposome with a flower-like conformation after protein interaction. Both experiments were repeated three times.

To gain further information on the interaction, RICS experiments were performed by adding 36 μM micelles labelled with $Alexa_{488}$ (13 nM) to unstained giant vesicles to a final pH of 5.3. Changes in diffusion coefficient were monitored. Before casein addition, liposomes are only visible in the transmission channel, while upon interaction with casein, fluorescence is observed at the membrane.

In Fig.4.a) is reported the schematic representation of POPC:POPG model membranes added of fluorescent micelles samples. In Fig.4.b) we report RICS analysis: 256 × 256 pixel size representative images of liposomes in presence of $Alexa_{488}$-micelles, where coloured squares represent 64 × 64 pixel regions of interest (ROIs) where the analysis was performed. Corresponding spatial correlation functions and fits are also shown in Fig.4.c), calculated also in this case with immobile subtraction (MAV = 10). By analysing different ROIs in the image, we are able to disentangle the contribution of freely diffusing casein structures in solution away from the membrane and casein molecules in close proximity or interacting with the membrane. The diffusion coefficient distributions of casein diffusing in solution, casein aggregated and casein that interacted with liposomes are shown in Fig.4.b). After casein sample addition, the measured diffusion coefficient in ROIs away from liposome's membrane is variable and ranging from 17 $\mu m^2/s$ to 65 $\mu m^2/s$, being comparable with data in Fig.2.c). These data suggest that a disassembly of the micelles occurs and that α-casein are likely to assume the same state as the one measured at the same pH in the absence of membranes. A certain fraction of protein then interacts with liposomes. The measured diffusion coefficient at the membrane drops to lower values 6 ± 2 $\mu m^2/s$. This value is distinguishable from diffusion coefficients reported for protein aggregates (2 ± 1 μm^2 /s) found in the absence of liposomes which are also found in this sample (see supplementary Fig.S3 for large field images).

Control RICS experiments were performed adding casein dissolved at pH 5.3 solution to liposomes. Measurements reveal that fluorescence signal is homogeneously dispersed, liposomes are not visible and the diffusion coefficient calculated for casein in these conditions is 50 ± 10 $\mu m^2/s$ (supplementary Fig.S4). This is in somehow

expected because, according to the literature, only small limited changes in protein structure are likely to occur[17].

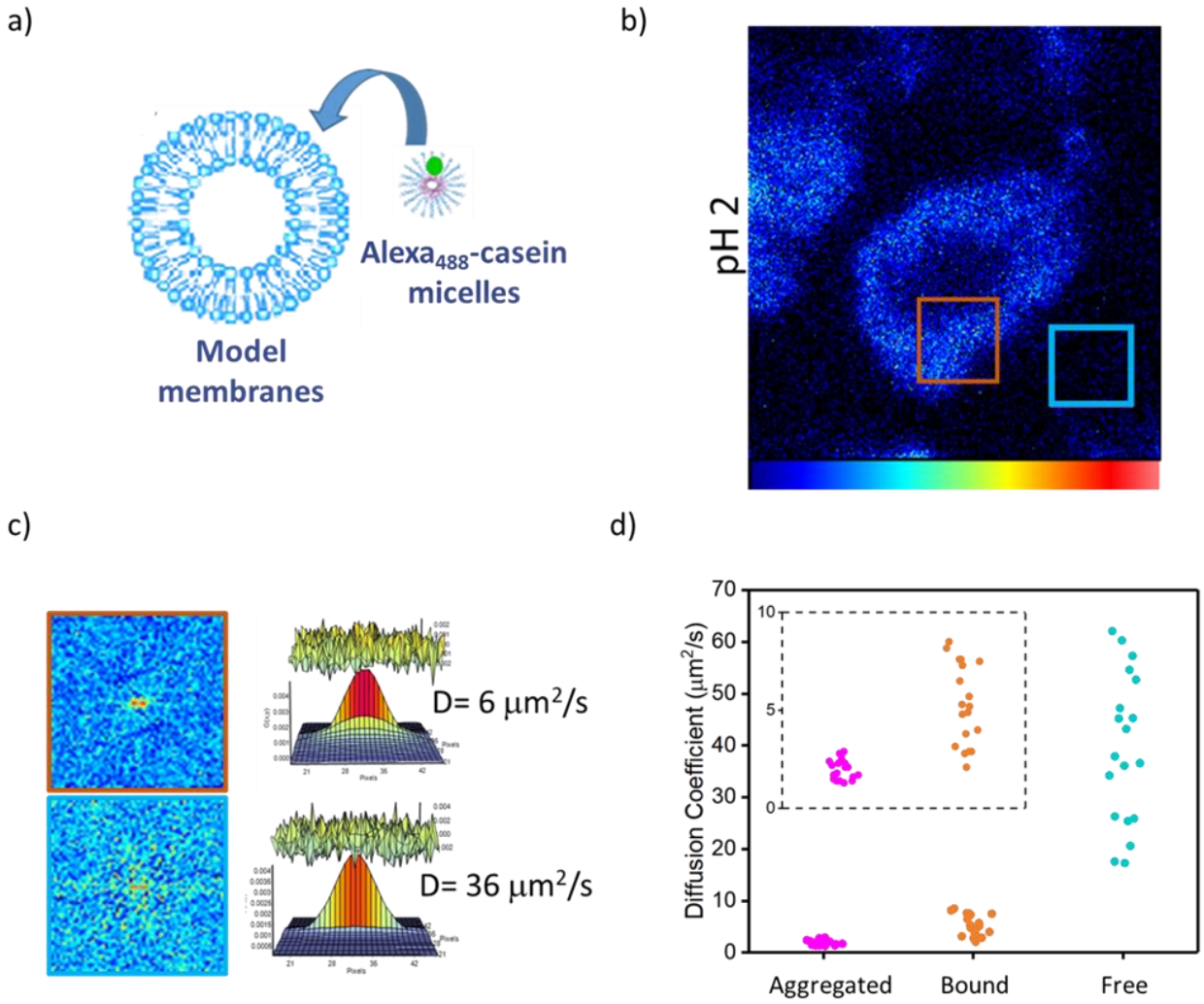

Fig. 4 (a) Schematic representation of α-casein micelles (36 μM, pH 2) stained with $Alexa_{488}$ and POPC:POPG model membrane. (b) 256 × 256 representative confocal images of liposomes interacting with casein in which coloured squares represent 64 x 64 ROIs where RICS measurements are performed. (c) Spatial autocorrelation functions, with subtraction of the immobile fraction using MAV = 10, and relative fits, spatial correlation function is marked with the same colour of the ROI in which they are calculated. (d) Diffusion coefficients distributions of casein in its different states (free, aggregated and bound to liposomes). The experiment was repeated four times.

Interestingly, if the same experiment is repeated in conditions where the protein starts from its native like state at pH 7 only minor changes are observed. In Fig.5 the RICS analysis of a sample containing non stained liposomes is reported after the addition of 36 μM α-casein pH 7 labelled with 13 nM $Alexa_{488}$. Final pH of this sample is pH 5.3 as before. In panel 5.a) a representative fluorescence intensity image is reported

where no structure with size above the optical resolution are observed. The correlation function and respective fit are also reported whose analysis gives back a diffusion coefficient of 47 ± 10 $\mu m^2/s$, which is compatible with the presence of native protein diffusing together with small oligomers, which may be formed due to the loss of electrostatic interactions. Interestingly, in this case, the liposomes are only visible in the transmission channel (Fig.5.b)), no significant fluorescence signal is observed at their surface and their morphology remains unvaried. This clearly indicates that, in the observed conditions, no significant interaction occurs.

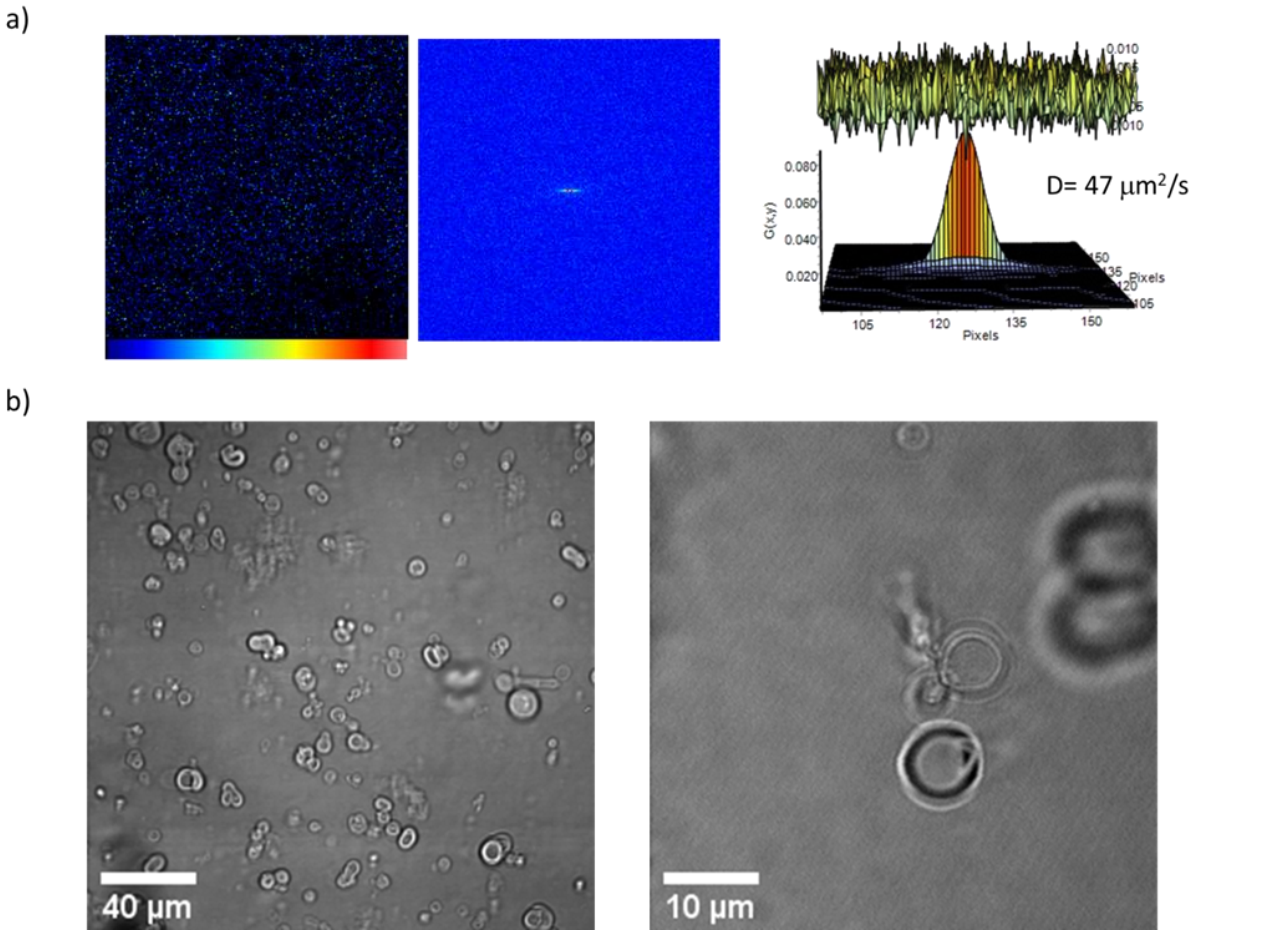

Fig. 5 (a) RICS analysis: right column: 256 × 256 pixel representative confocal images of liposomes added of α-casein-$Alexa_{488}$ (36 μM, pH 7). Final pH is brought to 5.3 value. Left column: spatial autocorrelation functions and relative fits. (b) representative images of POPC:POPG liposomes in the transmission channel. The liposomes are visible only in transmission channel indicating that no interaction occurs between protein and membrane. The experiment was repeated twice.

At pH 5.3, liposomes are negatively charged and the protein has a negligible charge disfavouring both aggregation and protein adhesion to lipids. Summarising these results, it is possible to state that α-casein interactions with membranes, in conditions where the net charge of the protein is reduced close to zero by a sudden change in pH is regulated by the initial state of the protein.

Conclusions

The action of a protein in cellular environment is dictated by its structure and environmental conditions. Among the other effects, during protein trafficking and diffusion within a cell environment, a protein may experience pH changes, which regulate its macromolecular properties such as the stability and activity, being these two last not necessarily disentangled. The comprehension of the different association/aggregation states of proteins and the evaluation of their behaviour in presence of lipid membranes is essential to elucidate the basis of functional and pathological protein-membrane interactions.

Here we present results on α-casein protein, which clearly put in evidence that its interaction with membranes in a specific environment has a memory of the initial state of the protein molecule i.e. the initial conformational/structural properties of the protein regulate the fate of the interacting molecules.

In this study, we have highlighted the ability of α-casein to form small micelles at acidic pH. In this assembly state, protein secondary structures is mainly characterised by intermolecular β-sheets. At pH 7, as expected, the protein is in its native like state with secondary structure presenting a high content of α–helices and random coils. A main difference between these two protein states also consists in the interaction with the hydrophobic dyes Pyrene and ANS, being the protein at pH 2 the one with larger affinity to both dyes. Once α-casein micelles are dissolved at pH values close to the isoelectric point in absence and in presence of membranes, micelles undergo a partial disassembly process accompanied by disordered aggregation into amorphous structures (both oligomers and large micron-scale aggregates). At pH 7, when the initial state of the protein is native like, the change of pH to the isoelectric point only induces slight modifications in the diffusion coefficient. Results also show a different effect of the two samples on POPC:POPG GVs, demonstrating that only proteins

initially in their micellar state are able to interact with the POPC:POPG GVs in liquid disordered phase inducing severe morphological changes, dehydration and increasing the rigidity of the lipid bilayer. This is possibly due to highly reactive hydrophobic species generated during the abrupt pH change causing micelles disassembly. α-casein molecules are able to quickly form large aggregates or to interact with membrane bilayers. Interestingly α-casein membrane co-aggregates are formed with a flower-like shape that, to our knowledge, was not previously observed in the literature as a result of protein-membrane interactions. Protein is localised in the external part and its insertion in membrane layers is likely to exclude water, increasing the rigidity of the lipid membranes in the regions were the protein is present. Our results highlight that the solvent conditions and their variations not only affect conformational and supramolecular state of proteins but also the interaction with lipids and hence their activity. Presented data contribute to a deeper understanding of protein interaction with membranes upon controlled regulation by micro-environmental properties. The coupling between spectroscopy and microscopy measurements added important information in the analysis of heterogeneous samples making possible to follow dynamic events, at molecular level and in real time.

Author contribution

SA Investigation, Data analysis, Methodology, Writing & editing, Data curation, Visualization. GS Methodology, Validation Writing & editing, Data curation, Visualization. VF Validation, funding acquisition, Resources - review & editing. VV Conceptualization, Methodology, Validation, Investigation, Formal analysis, Supervision, Writing - original draft, Writing - review & editing, Project administration, Funding acquisition, Resources.

Acknowledgements

The authors thank the University of Palermo for financial support (FFR – PROMETA project). GS has received funding from PON AIM1809078-1. RICS analysis was performed at the “Bioimaging and Dosimetry lab”—Advanced Technologies Network (ATeN) Center, University of Palermo

Bibliography

1. Relini A, Marano N, Gliozzi A. Misfolding of Amyloidogenic Proteins and Their Interactions with Membranes. *Biomolecules*. 2014;4(1):20. doi:10.3390/BIOM4010020

2. Relini A, Cavalleri O, Rolandi R, Gliozzi A. The two-fold aspect of the interplay of amyloidogenic proteins with lipid membranes. *Chem Phys Lipids*. 2009;158(1):1-9. doi:10.1016/J.CHEMPHYSLIP.2008.11.003

3. Le Parc A, Leonil J, Chanat E. αS1-casein, which is essential for efficient ER-to-Golgi casein transport, is also present in a tightly membrane-associated form. *BMC Cell Biol*. 2010;11:65. doi:10.1186/1471-2121-11-65

4. Zhang X, Ge N, Keiderling TA. Electrostatic and Hydrophobic Interactions Governing the Interaction and Binding of β-Lactoglobulin to Membranes†. *Biochemistry*. 2007;46(17):5252-5260. doi:10.1021/BI602483P

5. Gawrisch K, Barry JA, Holte LL, Sinnwell T, Bergelson LD, Ferretti JA. Role of interactions at the lipid-water interface for domain formation. *http://dx.doi.org/103109/09687689509038500*. 2009;12(1):83-88. doi:10.3109/09687689509038500

6. Chenal A, Vernier G, Savarin P, et al. Conformational States and Thermodynamics of α-Lactalbumin Bound to Membranes: A Case Study of the Effects of pH, Calcium, Lipid Membrane Curvature and Charge. *J Mol Biol*. 2005;349(4):890-905. doi:10.1016/J.JMB.2005.04.036

7. Mitranic MM, Pâquet MR, Moscarello MA. The interaction of bovine milk galactosyltransferase with lipid and alpha-lactalbumin. *Biochim Biophys Acta*. 1988;956(3):277-284. doi:10.1016/0167-4838(88)90144-6

8. Carver JA, Holt C. Functional and dysfunctional folding, association and aggregation of caseins. *Adv Protein Chem Struct Biol*. 2019;118:163-216. doi:10.1016/BS.APCSB.2019.09.002

9. Bhat MY, Dar TA, RajendrakumarSingh L. Casein Proteins: Structural and Functional Aspects. *Milk Proteins - From Struct to Biol Prop Heal Asp*. September 2016. doi:10.5772/64187

10. McMahon DJ, Brown RJ. Composition, Structure, and Integrity of Casein Micelles: A Review. *J Dairy Sci*. 1984;67(3):499-512. doi:10.3168/JDS.S0022-0302(84)81332-6

11. Głąb TK, Boratyński J. Potential of Casein as a Carrier for Biologically Active Agents. *Top Curr Chem*. 2017;375(4). doi:10.1007/S41061-017-0158-Z

12. Mcmahon DJ, Brown RJ. Composition, Structure, and Integrity of Casein Micelles" A Review 1. *J Dairy Sci*. 67:499-512. doi:10.3168/jds.S0022-0302(84)81332-6

13. Crespo-Villanueva A, Gumí-Audenis B, Sanz F, et al. Casein interaction with lipid membranes: Are the phase state or charge density of the phospholipids affecting protein adsorption? *Biochim Biophys Acta - Biomembr*. 2018;1860(12):2588-2598. doi:10.1016/J.BBAMEM.2018.09.016

14. Le Parc A, Leonil J, Chanat E. αS1-casein, which is essential for efficient ER-to-Golgi casein transport, is also present in a tightly membrane-associated form. *BMC Cell Biol*. 2010;11:65. doi:10.1186/1471-2121-11-65

15. Farrel HM., Jmenez-Flores R., Bleck GT., et al. Nomenclature of the Proteins of Cows' Milk-Sixth Revision | Elsevier Enhanced Reader. J. Dairy Sci . https://reader.elsevier.com/reader/sd/pii/S0022030204733196?token=45F9FA55A5B81F3C7332721B575E97A9926E96176D8B370B8FCD207E73C8B3F6182470288CABBF6E06F3983BE2DDFCE1&originRegion=eu-west-1&originCreation=20220210121153. Published 2004. Accessed February 10, 2022.

16. Sinaga H, Bansal N, Bhandari B. Effects of milk pH alteration on casein micelle size and gelation properties of milk. *http://dx.doi.org/101080/1094291220161152480*. 2016;20(1):179-197. doi:10.1080/10942912.2016.1152480

17. Chakraborty A, Basak S. pH-induced structural transitions of caseins. *J Photochem Photobiol B Biol*. 2007;87(3):191-199. doi:10.1016/J.JPHOTOBIOL.2007.04.004

18. Liu Y, Guo R. pH-dependent structures and properties of casein micelles. *Biophys Chem*. 2008;136(2-3):67-73. doi:10.1016/J.BPC.2008.03.012

19. McMahon DJ, Oommen BS. Casein Micelle Structure, Functions, and Interactions. *Adv Dairy Chem Vol 1A Proteins Basic Asp 4th Ed*. January 2013:185-209. doi:10.1007/978-1-4614-4714-6_6

20. Holt C, Carver JA. Quantitative multivalent binding model of the structure, size distribution and composition of the casein micelles of cow milk. *Int Dairy J*. 2022;126:105292. doi:10.1016/J.IDAIRYJ.2021.105292

21. Huppertz T, Vaia B, Smiddy MA. Reformation of casein particles from alkaline-disrupted casein micelles. *J Dairy Res*. 2008;75(1):44-47. doi:10.1017/S0022029907002956

22. Odagiri S, Nickerson TA. MICELLAR CHANGES IN SKIMMILK TREATED WITH ALKALI OR ACID. doi:10.3168/jds.S0022-0302(65)88419-3

23. Madadlou A, Mousavi ME, Emam-Djomeh Z, Sheehan D, Ehsani M. Alkaline pH does not disrupt re-assembled casein micelles. *Food Chem*. 2009;116(4):929-932. doi:10.1016/J.FOODCHEM.2009.03.048

24. Clermont Y, Xia L, Rambourg A, Turner JD, Hermo L. Transport of casein submicelles and formation of secretion granules in the Golgi apparatus of epithelial cells of the lactating mammary gland of the rat. *Anat Rec*. 1993;235(3):363-373. doi:10.1002/AR.1092350305

25. Rehan F, Ahemad N, Gupta M. Casein nanomicelle as an emerging biomaterial—A comprehensive review. *Colloids Surfaces B Biointerfaces*. 2019;179:280-292. doi:10.1016/J.COLSURFB.2019.03.051

26. Gandhi S, Roy I. Doxorubicin-loaded casein nanoparticles for drug delivery: Preparation, characterization and in vitro evaluation. *Int J Biol Macromol*. 2019;121:6-12. doi:10.1016/J.IJBIOMAC.2018.10.005

27. Sahu A, Kasoju N, Bora U. Fluorescence Study of the Curcumin−Casein Micelle Complexation and Its Application as a Drug Nanocarrier to Cancer Cells. *Biomacromolecules*. 2008;9(10):2905-2912. doi:10.1021/BM800683F

28. Semo E, Kesselman E, Danino D, Livney YD. Casein micelle as a natural nano-capsular vehicle for nutraceuticals. *Food Hydrocoll 21*. 2007:936-942. doi:10.1016/j.foodhyd.2006.09.006

29. Farrell HM, Cooke PH, Wickham ED, Piotrowski EG, Hoagland PD. Environmental influences on bovine κ-casein: Reduction and conversion to fibrillar (amyloid) structures. *J Protein Chem*. 2003;22(3):259-273. doi:10.1023/A:1025020503769

30. Thorn DC, Ecroyd H, Sunde M, Poon S, Carver JA. Amyloid fibril formation by bovine milk alpha s2-casein occurs under physiological conditions yet is prevented by its natural counterpart, alpha s1-casein. *Biochemistry*. 2008;47(12):3926-3936. doi:10.1021/BI701278C

31. Thorn DC, Meehan S, Sunde M, et al. Amyloid Fibril Formation by Bovine Milk κ-Casein and Its Inhibition by the Molecular Chaperones αS- and β-Casein†. *Biochemistry*. 2005;44(51):17027-17036. doi:10.1021/BI051352R

32. Recio I, Visser S. Identification of two distinct antibacterial domains within the sequence of bovine αs2-casein. *Biochim Biophys Acta - Gen Subj*. 1999;1428(2-3):314-326. doi:10.1016/S0304-

4165(99)00079-3

33. McCann KB, Shiell BJ, Michalski WP, et al. Isolation and characterisation of a novel antibacterial peptide from bovine αS1-casein. *Int Dairy J*. 2006;16(4):316-323. doi:10.1016/J.IDAIRYJ.2005.05.005

34. De Luca G, Fennema Galparsoro D, Sancataldo G, Leone M, Foderà V, Vetri V. Probing ensemble polymorphism and single aggregate structural heterogeneity in insulin amyloid self-assembly. *J Colloid Interface Sci*. 2020;574:229-240. doi:10.1016/J.JCIS.2020.03.107

35. Librizzi F, Carrotta R, Spigolon D, Bulone D, San Biagio PL. α-Casein Inhibits Insulin Amyloid Formation by Preventing the Onset of Secondary Nucleation Processes. *J Phys Chem Lett*. 2014;5(17):3043-3048. doi:10.1021/JZ501570M

36. Parasassi T, De Stasio G, d'Ubaldo A, Gratton E. Phase fluctuation in phospholipid membranes revealed by Laurdan fluorescence. *Biophys J*. 1990;57(6):1179-1186. doi:10.1016/S0006-3495(90)82637-0

37. Sanchez SA, Tricerri MA, Gunther G, Gratton E. Laurdan Generalized Polarization: from cuvette to microscope. 2007.

38. Parasassi T, Krasnowska EK, Bagatolli L, Gratton E. Laurdan and Prodan as Polarity-Sensitive Fluorescent Membrane Probes. *J Fluoresc*. 1998;8(4):365-373. doi:10.1023/A:1020528716621

39. Galparsoro DF, Zhou X, Jaaloul A, Piccirilli F, Vetri V, Foderà V. Conformational Transitions upon Maturation Rule Surface and pH-Responsiveness of α-Lactalbumin Microparticulates. *ACS Appl Bio Mater*. 2021;4(2):1876-1887. doi:10.1021/ACSABM.0C01541

40. Kapusta P. Absolute Diffusion Coefficients: Compilation of Reference Data for FCS Calibration. 2010. doi:10.1209/0295-5075/83/46001

41. Sadiq U, Gill H, Chandrapala J. Casein Micelles as an Emerging Delivery System for Bioactive Food Components. *Foods*. 2021;10(8). doi:10.3390/FOODS10081965

42. Vetri V, Ossato G, Militello V, Digman MA, Leone M, Gratton E. Fluctuation methods to study protein aggregation in live cells: Concanavalin a oligomers formation. *Biophys J*. 2011;100(3):774-783. doi:10.1016/j.bpj.2010.11.089

43. Digman MA, Sengupta P, Wiseman PW, Brown CM, Horwitz AR, Gratton E. Fluctuation Correlation Spectroscopy with a Laser-Scanning Microscope: Exploiting the Hidden Time Structure. *Biophys J*. 2005;88(5):L33. doi:10.1529/BIOPHYSJ.105.061788

44. Dodero VI, Quirolo ZB, Sequeira MA. Biomolecular studies by circular dichroism . *Front Biosci*. 2011;16:61.

45. Chanat E, Martin P, Ollivier-Bousquet M. Alpha(S1)-casein is required for the efficient transport of beta- and kappa-casein from the endoplasmic reticulum to the Golgi apparatus of mammary epithelial cells. *J Cell Sci*. 1999;112 (Pt 19)(19):3399-3412. doi:10.1242/JCS.112.19.3399

46. Wu MM, Llopis J, Adams S, et al. Organelle pH studies using targeted avidin and fluorescein–biotin. *Chem Biol*. 2000;7(3):197-209. doi:10.1016/S1074-5521(00)00088-0

47. Semisotnov G V., Rodionova NA, Razgulyaev OI, Uversky VN, Gripas' AF, Gilmanshin RI. Study of the "molten globule" intermediate state in protein folding by a hydrophobic fluorescent probe. *Biopolymers*. 1991;31(1):119-128. doi:10.1002/BIP.360310111

48. Paroutis P, Touret N, Grinstein S. The pH of the secretory pathway: measurement, determinants, and regulation. *Physiology (Bethesda)*. 2004;19(4):207-215. doi:10.1152/PHYSIOL.00005.2004

49. Le Parc A, Leonil J, Chanat E. αS1-casein, which is essential for efficient ER-to-Golgi casein transport,

is also present in a tightly membrane-associated form. *BMC Cell Biol*. 2010;11(1):1-15. doi:10.1186/1471-2121-11-65/FIGURES/7

50. Van Maarschalkerweerd A, Vetri V, Vestergaard B. Cholesterol facilitates interactions between α-synuclein oligomers and charge-neutral membranes. *FEBS Lett*. 2015;589(19):2661-2667. doi:10.1016/j.febslet.2015.08.013

51. Anselmo S, Sancataldo G, Mørck Nielsen H, Foderà V, Vetri V. Peptide-Membrane Interactions Monitored by Fluorescence Lifetime Imaging: A Study Case of Transportan 10. *Langmuir*. 2021;37(44):13148-13159. doi:10.1021/ACS.LANGMUIR.1C02392/SUPPL_FILE/LA1C02392_SI_001.PDF

52. Rao E, Foderà V, Leone M, Vetri V. Direct observation of alpha-lactalbumin, adsorption and incorporation into lipid membrane and formation of lipid/protein hybrid structures. *Biochim Biophys Acta - Gen Subj*. 2019;1863(5):784-794. doi:10.1016/j.bbagen.2019.02.005